Electronic Supplementary Information

Tailoring sensitization properties and improving near-infrared to visible photon upconversion performance through alloying in superatomic molecular Au_{25} nanoclusters

Masaaki Mitsui,* Yuki Miyoshi, Daichi Arima

Department of Chemistry, College of Science, Rikkyo University, 3-34-1, Nishiikebukuro, Toshima-ku, Tokyo, 171-8501, Japan.

Corresponding author

*E-mail: mitsui@rikkyo.ac.jp

Contents

1. Reagents

Hydrogen tetrachloroaurate(III) tetrahydrate ($HAuCl_4 \cdot 4H_2O$, 99.0%); copper(II) nitrate trihydrate ($Cu(NO_3)_2 \cdot H_2O$, 99.8+%); tetrahydrofuran (THF, 99.8%); triphenylphosphine (PPh_3, 97.0+%); and dichloromethane (DCM, 99.5+%) were purchased from FUJIFILM Wako Pure Chemical Corp. Sodium borohydride ($NaBH_4$, >95.0%); 2-phenylethanethiol; 3,3'-diethylthiatricarbocyanine iodide (CyS7, >98.0%); perylene (>99.0%, purified by sublimation); 9,10-diphenylanthracene (DPA, >99.0%, purified by sublimation); 9,10-bis(phenylethynyl)anthracene (BPEA, >98.0%); and tetracene (>99.0%, purified by sublimation) were purchased from Tokyo Chemical Industry Co., Ltd. Sodium hexafluoroantimonate(V) ($NaSbF_6$, 99%) was purchased from Fluorochem Ltd. Toluene (99.5%); acetone (99.5%); methanol (≥ 99.8%); ethanol (99.5%); *n*-hexane; rubrene (99.99%); and *N*,*N*'-bis(2,5-di-*tert*-butylphenyl)-3,4,9,10-perylenedicarboximide (^{t}Bu-PDI, 97%) were purchased from Sigma-Aldrich Co. LLC. Ultrapure water (resistivity ≥ 18.2 MΩcm) was produced using a Direct-Q UV distillation system. All reagents were used as received.

2. Nanocluster Synthesis

Synthesis of Cu-$SPhC_2H_4$: Copper(II) nitrate trihydrate ($Cu(II)NO_3 \cdot 3H_2O$, 300 mg, 1.24 mmol) was dissolved in 10 mL of ethanol under ultrasonication to obtain a blue solution. To this solution, 2-phenylethanethiol (167 μL) was added under stirring, resulting in the immediate formation of a yellow solid. After stirring for 30 min, the crude yellow solid was collected by centrifugation. The obtained solid was washed twice with ethanol and eight times with *n*-hexane, followed by drying under vacuum for 20 minutes using a rotary evaporator to yield Cu-$SPhC_2H_4$.

Synthesis of $[Au_{25-x}Cu_x(PPh_3)_{10}(SPhC_2H_4)_5Cl_2](SbF_6)_2$: The synthesis of $[Au_{25-x}Cu_x(PPh_3)_{10}(SPhC_2H_4)_5Cl_2](SbF_6)_2$ was conducted by modifying previous report.[1] A solution of $HAuCl_4 \cdot 4H_2O$ (30 mM, 6.5 mL, 0.25 mmol) was evaporated to dryness under reduced pressure and the residue dissolved in 5 mL of ethanol. To this solution, a solution of PPh_3 (160 mg, 0.61 mmol) in 5 mL of ethanol was added under stirring, resulting in the formation of a white solid after initially turning colorless. A solution of $NaBH_4$ (19 mg, 0.50 mmol) in 3 mL of ethanol was then added dropwise over approximately one minute, changing the solution to a reddish-purple color. Subsequently, 5 mL of ethanol, containing the precursor complex Cu-$SPhC_2H_4$ (36 mg, 0.18 mmol), was added to the solution, resulting in a reddish-brown mixture accompanied by precipitation. The mixture was stirred vigorously at room temperature for 20 hours, followed by centrifugation and filtration through a membrane filter (pore size: 0.2 μm) to obtain a brown solution. An excess of $NaSbF_6$/ethanol solution was added, stirred, and the mixture was centrifuged to collect a crude product containing a dark green precipitate. The crude product was washed

1–2 times with H_2O and 8–10 times with *n*-hexane before being extracted with DCM. The extract was subjected to normal-phase column chromatography using DCM : methanol (100 : 1) as eluent to separate the desired product from the by-product $[Au_2(PPh_3)_2(SPhC_2H_4)]^+$, which can be identified by UV light detection on a TLC plate (Silica gel 60 F_{254}, Merck).

Synthesis of $[Au_{25}(PPh_3)_{10}(SPhC_2H_4)_5Cl_2](SbF_6)_2$: The synthesis of $[Au_{25}(PPh_3)_{10}(SPhC_2H_4)_5Cl_2]^{2+}$ (**Au_{25}-rod**) was conducted by adapting a previously reported method for producing ultrapure samples.[2] Initially, $HAuCl_4{\cdot}4H_2O$ (103.0 mg, 250 μmol) was dissolved in 8 mL of ethanol, to which PPh_3 (180 mg, 686 μmol) was added. The mixture was stirred at room temperature for 15 minutes, during which the solution's color changed from yellow to transparent, resulting in the formation of a white solid precipitate. Following this, the solvent was evaporated, and the white solid was redissolved in 8 mL of toluene. The addition of a $NaBH_4$ solution prepared in ethanol (26 mg in 5 mL) to this toluene mixture resulted in the solution turning black immediately. The mixture was then stirred for 2 hours, after which the solvent was removed under reduced pressure at 50 °C using a rotary evaporator, leaving a black-red solid. This solid was dissolved in 20 mL of DCM, and the solution was centrifuged to remove insoluble materials. To the clear solution, phenylethanethiol (300 μL) was added, and the reaction mixture was stirred in a thermostatic bath set at 40°C for 96 hours. To precipitate the crude product, an excess of *n*-hexane was added to the yellowish solution, and the supernatant was decanted. The crude product was washed five times with a *n*-hexane : DCM mixture (9 : 1, v/v), then redissolved in methanol. An excess of $NaSbF_6$ was added to precipitate the product, and the supernatant was removed. After evaporating the solvent, the product was washed with a methanol : water mixture (2 : 8, v/v) to yield the desired product.

3. Electrospray Ionization Time-of-Flight Mass Spectrometry

The synthesized nanoclusters (NCs) were characterized using electrospray ionization time-of-flight mass spectrometry (JEOL, JMS-T100LP AccuTOF LC-Plus). For the analysis, the NCs were dissolved in methanol and introduced into the mass spectrometer in positive-ion mode. Mass calibration was performed using a solution of NaI in methanol as the standard. The positive-ion mode ESI-TOF-mass spectrum of the resultant products exhibited a series of NC peaks, each containing different numbers of Cu atoms (x = 0–10). For example, as shown in Fig. S1, the peak at 3685.0 m/z corresponds to the mass of $[Au_{18}Cu_7(PPh_3)_{10}(S\text{-}C_2H_4Ph)_5Cl_2]^{2+}$ (3685.0 m/z). The isotope pattern of the peak closely matched the theoretically obtained one, confirming the successful synthesis of the intended product.

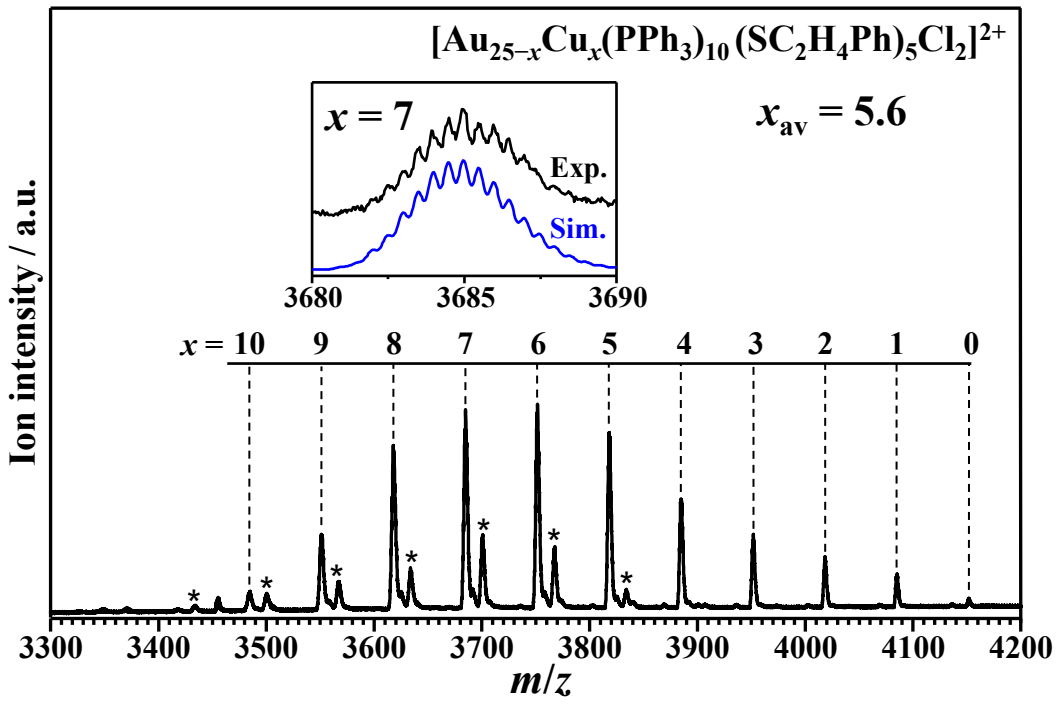

Fig. S1 Positive-ion electrospray ionization mass spectrum of the prepared $[Au_{25-x}Cu_x(PPh_3)_{10}(S\text{-}C_2H_4Ph)_5Cl_2]^{2+}$ (**AuCu-rod**) nanoclusters (x_{ave} = 5.6). Inset shows experimental (black) and simulated (blue) isotopic patterns of x = 7. A series of peaks under the asterisk label were assigned to compositions in which one of the S-C_2H_4Ph ligands was replaced by a Cl atom, i.e., $[Au_{25-x}Cu_x(PPh_3)_{10}(S\text{-}C_2H_4Ph)_4Cl_3]^{2+}$.

4. Spectroscopic and Electrochemical Measurements

The ultraviolet–visible (UV–vis) absorption spectra were obtained using a Lambda 650 spectrometer (Perkin-Elmer) or V-630 spectrometer (Jasco) across a wavelength range of 300–1000 nm at 1 nm intervals. The setup for emission spectroscopy has been detailed in previous publications.[3,4] Briefly, emission spectra were acquired utilizing either a fiber optics CCD spectrometer (USB4000, Ocean optics) or a liquid nitrogen-cooled charge-coupled device camera (Spec-10:100B/LN, Roper Scientific). Continuous-wave lasers at 488, 532, and 805 nm served as the sources for photoexcitation. For the measurement of emission decays, picosecond pulsed lasers at 478-nm or 634-nm, with a pulse width of 40–80 ps (PiL048X or PiL063X, Advanced Laser Diode System) was utilized as the excitation source. The emission decay profiles were acquired using a system that combines the mentioned pulsed laser sources with an avalanche photodiode (APD, SPCM-AQRH-61, Perkin-Elmer) photon detector and a time-correlated single photon counting (TC-SPC) card (TimeHarp 260, PicoQuant). The analysis of decay

profiles was conducted using SymPhoTime 64 software (PicoQuant). Unless otherwise noted, all absorption and emission measurements were carried out in THF solutions, which were fully degassed using high-purity argon gas (> 99.999%).

Transient absorption (TA) spectroscopy measurements were conducted using a subnanosecond TA spectroscopy system (picoTAS, UNISOKU Co., Ltd.).[5] The pump source utilized was a picosecond Nd:YAG laser (355 nm, EKSPLA PL-2210A, 1 kHz, full width at half maximum (fwhm) = 25 ps) equipped with an optical parametric generator (EKSPLA PT400, 410−700 nm, 50 μJ/pulse @500 nm). The probe light source was a supercontinuum radiation source (INDUS FORTE 400, Leukos, 20 MHz, fwhm = 50–100 ps, 410–2400 nm). The time resolution of the system was estimated to be 80–100 ps at a 10−90% rise time. Measurements were performed in a quartz cell with a 2 mm optical path length.

To evaluate the oxidation potential of **AuCu-rod**, differential pulse voltammetry (DPV) measurements were conducted using ECstat-301 (EC Frontier Co., Ltd) at 0℃. In DPV measurements, deaerated DCM was employed as the solvent, and tetrabutylammonium perchlorate was used as the supporting electrolyte. A glassy carbon electrode was utilized as the working electrode, while a Pt wire served as the counter electrode. Ag/Ag^+ was employed as the reference electrode, and the internal standard was calibrated using the ferrocene/ferrocenium (Fc/Fc^+) redox couple. The scan rate of the electrode was set at 50 mVs^{-1}, and all measurements were performed using well-polished glassy carbon electrodes prior to each measurement.

5. Free Energy Changes for Charger Transfer (ΔG_{CT})

Free energy changes (ΔG_{CT}) of electron transfer from **AuCu-rod** to O_2 can be calculated by the Rehm−Weller equation: [10]

$$\Delta G_{\mathrm{CT}} = F\left[E_{AuCu}^{\mathrm{ox}} - E_{O_2}^{\mathrm{red}}\right] - E_{\mathrm{T}} + C, \qquad (S1)$$

where F is the Faraday constant, E_{AuCu}^{ox} and $E_{O_2}^{\mathrm{red}}$ are redox potentials of **AuCu-rod** (donor) and O_2 (acceptor), E_{T} is triplet state energy of **AuCu-rod** and C is coulombic interaction energy. The coulombic energy can be estimated by following equation: [11]

$$C = -\frac{z_{AuCu}^2 e^2}{\varepsilon_s\left(R_{AuCu} + R_{O_2}\right)} - \frac{e^2}{2}\left(\frac{z_{AuCu}^2}{R_{AuCu}} + \frac{1}{R_{O_2}}\right)\left(\frac{1}{\varepsilon_{ref}} - \frac{1}{\varepsilon_s}\right), \qquad (S2)$$

where z_{AuCu} represents the charge on **AuCu-rod** in the encounter complex (i.e., z_{AuCu} = +3), e is the elementary charge, ε_s and ε_{ref} are the dielectric constants of the solvent used in the absorption/emission measurements and used in electrochemical measurements, respectively. R is the van der Waals radii of **AuCu-rod** and O_2. The parameters used to calculate the ΔG_{CT} value between **AuCu-rod** and O_2 are summarized in Table S1.

Table S1. Free energy change of electron transfer from AuCu-rod to O_2 in THF estimated using the Rehm–Weller equation.

		R / nm	ε_{ref} [b]	ε_s [b]	E^{ox}_{donnor} / V vs. NHE	$E^{red}_{acceptor}$ / V vs. NHE	E_T / eV	C / eV	ΔG_{CT} /eV
Donor	**AuCu-rod**	9.48 [a]	8.93	7.58	+1.50	-	1.5	–0.21	+0.39
Acceptor	O_2	1.73	(DCM)	(THF)	-	–0.606	-		

[a] Obtained using reported crystal structures.[1] [b] Parentheses indicate the solvent used: dichloromethane (DCM) and tetrahydrofuran (THF). The redox potentials were converted to normal hydrogen electrode (NHE) potentials by +0.54 V for Ag/Ag^+ electrode reference.

6. Dynamic Light Scattering Measurements.

Dynamic light scattering measurements were performed using nanoSAQLA (Otsuka Electronics Co., Ltd.). Measurements were performed under ambient conditions, utilizing a 660 nm laser as the light source. The particle size distribution was evaluated by entering appropriate parameters, such as solvent viscosity and refractive index, into the dedicated software provided with the nanoSAQLA system and analyzing the second-order autocorrelation function $g^{(2)}(t)$ of the scattered light intensity. Measurements were conducted on a 20 mM BPEA/THF solution, matching the concentration conditions used for photon upconversion measurements. The scattering intensities of the 5 and 10 mM BPEA solutions were very weak and not stable due to the small amount of aggregates formed, making the particle size evaluation unreliable.

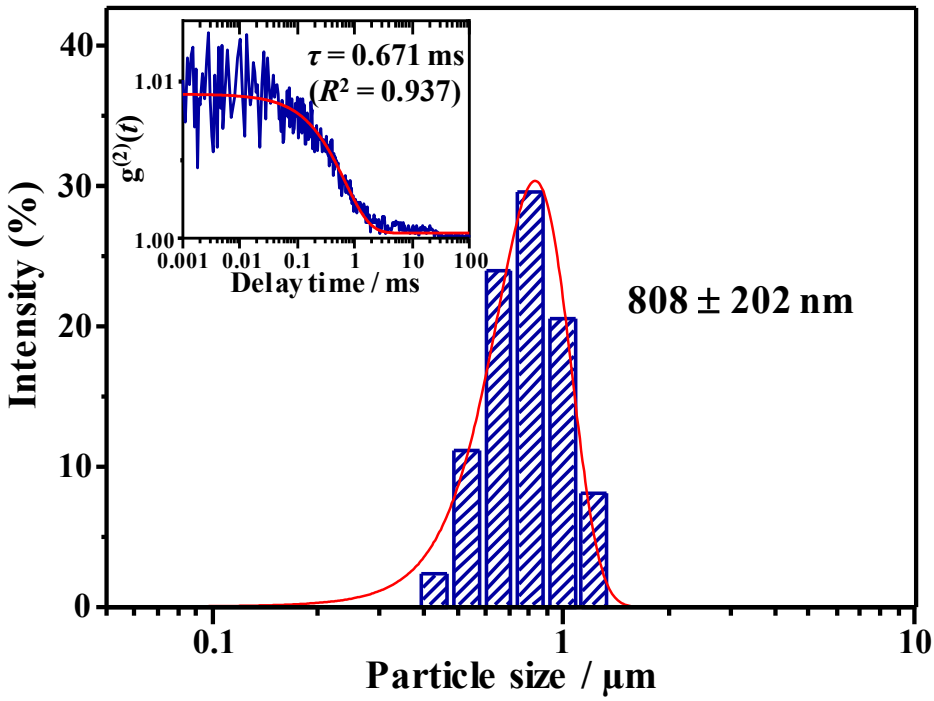

Fig. S2 The particle size distribution of BPEA aggregates was obtained from dynamic light scattering measurements of a THF solution with a BPEA concentration of 20 mM. The nanoparticles were not formed through a controlled process but rather in solution under conditions near or above the saturated solubility of BPEA in THF. Thus, the size distribution of the formed aggregates was influenced by the ambient temperature at the time of measurement.

7. Emission Quenching Experiments with Aromatic Acceptors

The determination of the rate constants of triplet energy transfer (k_{TET}) involved conducting quenching experiments on the emission lifetimes of the NCs, as described by the Stern-Volmer relationship as follows:

$$\frac{\tau_0}{\tau} = 1 + K_{SV}[Q] \qquad (S3)$$

where K_{SV} is the Stern−Volmer constant, [Q] is the acceptor concentration, and τ_0 and τ correspond to the unquenched and quenched emission lifetimes of the NCs, respectively. The results are summarized in Fig. S5 and Table S2.

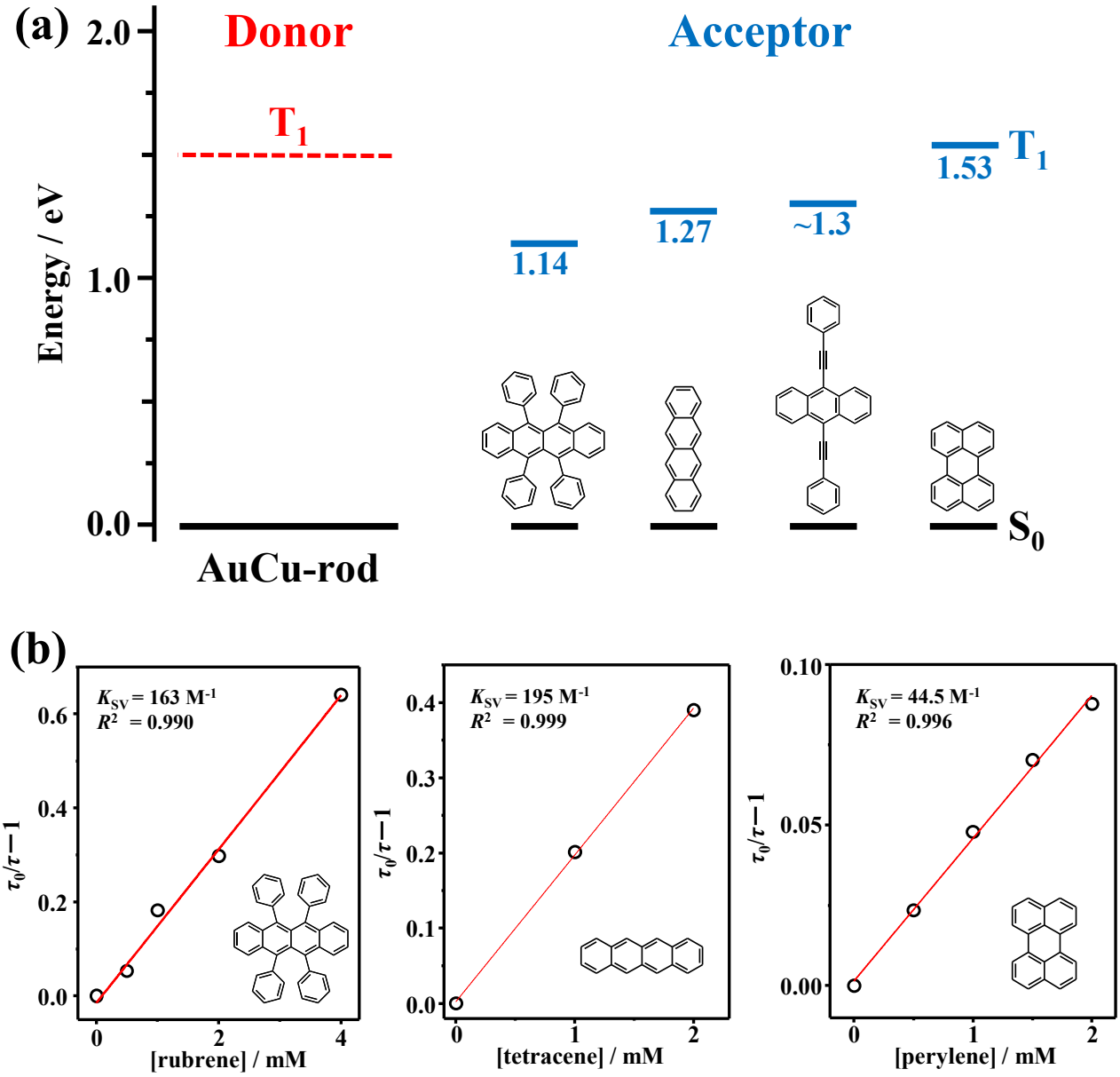

Fig. S3 (a) Energy level diagram showing the T_1 state energy region for combinations of **AuCu-rod** (donor) with four aromatic compounds (acceptors). (b) Stern–Volmer plot based on the emission lifetimes of a 20 μM **AuCu-rod** solution in deaerated THF, excited at 634 nm. The Stern-Volmer constant (K_{sv}) derived from a linear least-squares fit is also provided. Results for the BPEA acceptor are shown in Figs. 3e and 3f.

Table S2. **Phosphorescence quenching parameters of AuCu-rod obtained with different aromatic acceptors in deaerated THF (λ_{ex} = 634 nm).**

Donor	Acceptor	$E_{T(A)}$ / eV [a]	K_{SV} / M^{-1}	k_{TET} / $M^{-1}s^{-1}$
AuCu-rod	rubrene	1.14	163	5.9×10^7
	tetracene	1.27	195	6.3×10^7
	perylene	1.53	44.5	1.5×10^7

[a] Acceptor triplet state energies.

8 · Preparation of Sample Solutions for UC Measurements

A THF solution containing a mixture of **AuCu-rod** or **Au-rod** and BPEA was prepared in air. This solution was then transferred to a 1 cm quartz cuvette and thoroughly degassed under high purity argon gas (99.9999%). A 30 mM solution of BPEA in THF was prepared as the stock solution and sonicated at room temperature for 20 minutes. It was then diluted to the desired concentration, thoroughly mixed to ensure dissolution equilibrium. The achievement of dissolution equilibrium for BPEA was determined by the stabilization of the intensity ratio between monomer and aggregate emissions in the UC spectrum.

9. Evaluation of Internal UC Quantum Yield

The internal UC quantum yield Φ_{UCg} was determined by the relative method using the following equation:

$$\Phi_{UCg} = \frac{I_r\left(1-10^{-A_r(\lambda_{ex})}\right)\int F_o(\lambda_{em})d\lambda_{em} n_o^2}{I_o\left(1-10^{-A_o(\lambda_{ex})}\right)\int F_r(\lambda_{em})d\lambda_{em} n_r^2}\Phi_r \cdot \frac{1}{\Phi_{out}}, \quad (S4)$$

where subscripts "r" and "o" represent the reference and objective samples, Φ_r is the fluorescence quantum yield of the reference sample, I is the excitation light intensity used in the measurement, and n is the refractive index. $A(\lambda_{ex})$ and $F(\lambda_{em})$ represent the absorbance at the excitation wavelength, λ_{ex}, and the intensity at the emission wavelength, λ_{em}, respectively. Φ_{out} represents the outcoupling yield to compensate for the loss of upconverted photons due to reabsorption by sensitizer and emitter molecules. Importantly, when determining UC quantum yield at a NIR light excitation through the relative method, the choice of a reference dye is crucial. For example, if a dye excited at visible light, such as 532 nm, is used as the reference, the effect of chromatic aberration in the optical system can have a significant impact on the

value obtained. In this study, CyS7 dye, which can be excited at continuous-wave 805(±2)-nm laser (CivilLaser), was employed as a reference to eliminate such factors causing inaccuracies in the obtained Φ_{UCg} value. In addition, considering the significant difference in the wavelength range of the reference fluorescence and the observed UC emission, the intensity of the emission spectrum must be corrected by evaluating the spectral sensitivity characteristics of the instrument using a calibrated light source (HL-3P-INT-CAL, Ocean Photonics). It is particularly important to note that without performing this correction, the Φ_{UCg} value was overestimated by nearly five times.

Initially, the fluorescence quantum yield (Φ_f) of the CyS dye was evaluated using the detection system employed for the UC measurements, with 532 nm as the excitation light and ^{t}Bu-PDI ($\Phi_f = 0.97$ in toluene)[7] as the reference. By employing a relative method that disregards the Φ_{out} term in eqn (1), a result of 18.1% was obtained for CyS7 in ethanol. This value is somewhat lower than the Φ_f value of 22% reported for CyS7 in ethanol.[8] This discrepancy is considered to be due to the fact that the CCD spectrometer (USB4000, Ocean optics) used in this study is not sensitive to wavelengths longer than 900 nm. Thus, adopting the 18.1% obtained for the CyS7 reference dye as Φ_r in eqn (1), Φ_{UCg} was calculated. To enhance the statistical accuracy of the average value of Φ_{UCg}, the excitation light intensity was varied within the range that shows a linear dependency with a slope of 1 for the reference samples, and within the range where TTA occurs quasi-first-order for the objective samples. All these varied intensity data sets were then combined and inserted into eqn (S1), gaining more than 100 values of Φ_{UCg}. As shown in Fig. S2, a histogram of these values was fitted with a Gaussian function, resulting in the determination of the average and standard deviation of Φ_{UCg}.

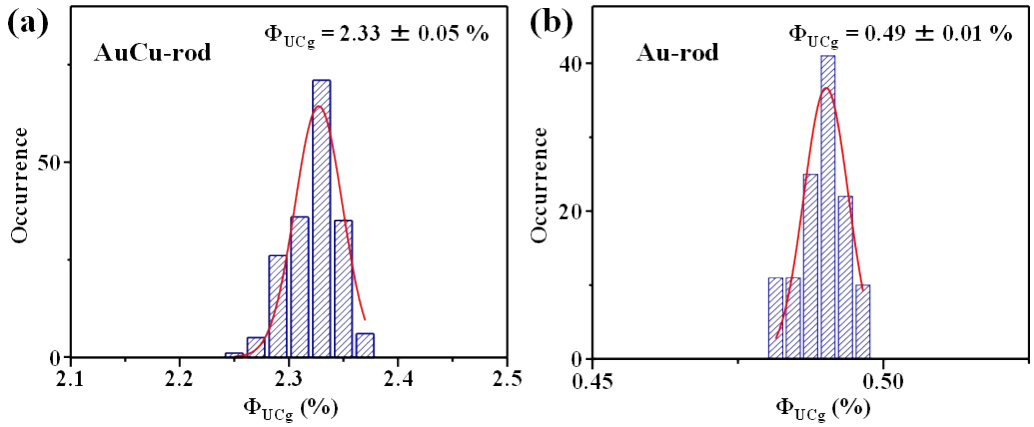

Fig. S4 Histograms of upconversion internal quantum yields (Φ_{UCg}) obtained for (a) 50 μM **AuCu-rod**/20 mM BPEA and (b) 50 μM **Au-rod**/20 mM BPEA pairs in deaerated THF.

The outcoupling yield (Φ_{out}) is defined as [9]

$$\Phi_{out} = \frac{\int F_0(\lambda) 10^{-\frac{A(\lambda)}{2}} d\lambda}{\int F_0(\lambda) d\lambda}, \quad (S5)$$

where $F_0(\lambda)$ is the emission intensity at wavelength λ at the excitation light focal point before reabsorption occurs, and $A(\lambda)$ is the absorbance of the UC solution at a wavelength λ, measured under an optical path length of 1.0 cm. In the UC measurement, since the excitation laser light passed through the center of the 1.0 × 1.0 cm cuvette, the optical path length for the emitted photons is 0.5 cm. Therefore, the actual emission intensity observed can be expressed as $F_0(\lambda)\cdot 10^{-A(\lambda)/2}$. It should be noted that in high-concentration BPEA solutions, UC emission from aggregates was observed in addition to the UC fluorescence of monomers (see Fig. 3d). Then, the $F_0(\lambda)$ spectrum was estimated through an inverse problem approach based on the actually measured UC spectrum ($F_{obs}(\lambda)$), as shown in Fig. S2. Initially, by dividing $F_{obs}(\lambda)$ by the transmission curve of the UC solution ($10^{-A(\lambda)/2}$), i.e., $F_{obs}(\lambda)\cdot 10^{A(\lambda)/2}$, we obtained the self-absorption corrected UC spectrum ($F_{long}(\lambda)$) in the wavelength region where UC emission was observed ($\lambda > 490$ nm). The no emission observed region at shorter wavelengths than $F_{long}(\lambda)$ ($\lambda < 490$ nm) is thought to be primarily composed of the monomer emission spectrum ($F_{short}(\lambda)$). Therefore, by adjusting the intensity of $F_{short}(\lambda)$ so that it smoothly connects with $F_{long}(\lambda)$, we created the $F_0(\lambda)$ spectrum. The spectrum obtained by $F_0(\lambda)\cdot 10^{-A(\lambda)/2}$ almost perfectly reproduced the $F_{obs}(\lambda)$ spectrum, indicating that the estimated $F_0(\lambda)$ spectrum is highly plausible. Substituting $F_0(\lambda)$ and $F_0(\lambda)\cdot 10^{-A(\lambda)/2}$ thus obtained into eqn (S2) to calculate Φ_{out} yielded a value of 0.31 for **AuCu-rod** (50 μM) and 0.22 for **Au-rod** (50 μM) with 20 mM BPEA.

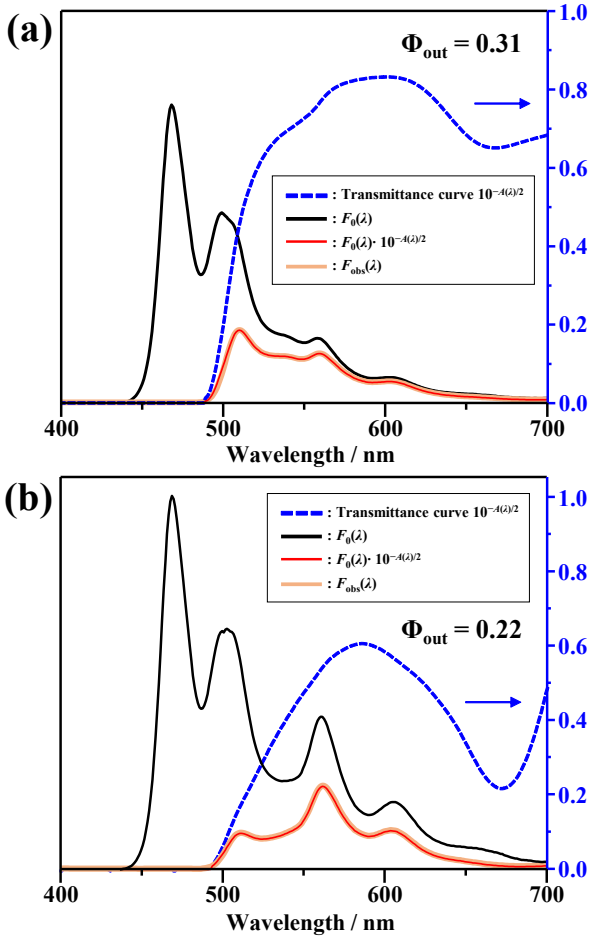

Fig. S5 Estimated original emission spectrum $F_0(\lambda)$ for a 20 mM BPEA in THF. Transmittance curve $10^{-A(\lambda)/2}$ (dashed line), self-absorption corrected UC spectra $F_0(\lambda)\cdot 10^{-A(\lambda)/2}$, and experimental UC spectra for (a) 50 μM AuCu-rod/20 mM BPEA and (b) 50 μM Au-rod/20 mM BPEA THF solutions. The Φ_{out} values, obtained from these data using eqn (S2), are also indicated.

10. Upconverted Emission Decay

Experimental setup details for recording upconverted emission delay profiles are elaborated in previous studies.[3,6,12] Briefly, a pseudo-pulse laser beam, generated through periodic blocking at 150 Hz by an optical chopper, was employed. Emission signals detected by an avalanche photodiode detector (APD410A/M, Thorlabs) were monitored with an oscilloscope (TBS1052C, Tektronix) and integrated using LabVIEW2020 developed software.

11. UC Threshold Intensity

The setup for studying the excitation intensity (I_{ex}) dependence on UC emission intensity (I_{UC}) is detailed in prior works.[3,6,12] Laser power was gauged by a power sensor-connected power meter (S120C, PM100, Thorlabs), adjusted incrementally via a variable neutral density filter. For UC measurements, the laser focused on the center of a 1.0 × 1.0 cm cuvette enabled excitation intensity calculation at the cuvette center as:

$$I_{ex} = \frac{P \cdot 10^{-A(\lambda_{ex})/2}}{\pi D^2/4}, \qquad (S6)$$

where D is the beam diameter. For the CW lasers at 532 nm and 805 nm, D was determined to be 0.060 cm and 0.18 cm, respectively, based on knife-edge measurements. The term $10^{-A(\lambda_{ex})/2}$ compensates for laser power attenuation over the 0.5 cm path to the cuvette center. UC emission was detected by an APD (SPCM50A/M) after filtration to eliminate other emissions and stray light. Background signal at each excitation intensity was subtracted from the emission intensity measured.

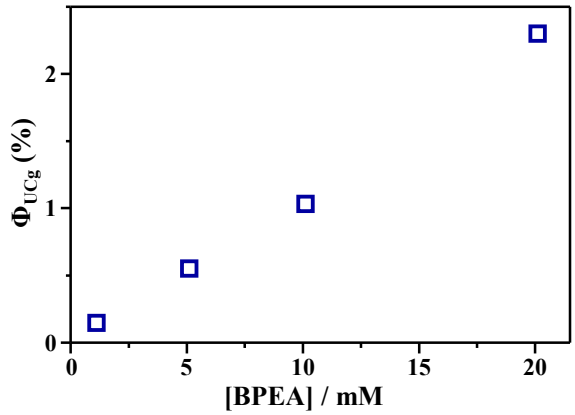

Fig. S6 BPEA concentration dependence of upconversion internal quantum yields (Φ_{UCg}) of **AuAc-rod** (50 μM) and BPEA (1–20 mM) mixtures in deaerated THF observed using a continuous wave 805-nm laser.

References

1) S. Yang, J. Chai, T. Chen, B. Rao, Y. Pan, H. Yu, M. Zhu, *Inorg. Chem.*, 2017, **56**, 1771−1774.
2) M. Galchenko, R. Schuster, A. Black, M. Riedner, C. Klinke, *Nanoscale* 2019, **11**, 1988−1994.
3) Y. Niihori, Y. Wada, and M. Mitsui, *Angew. Chem., Int. Ed.*, 2021, **60**, 2822–2827.
4) D. Arima, Y. Niihori, and M. Mitsui, *J. Mater. Chem. C*, 2022, **10**, 4597–4606.
5) T. Nakagawa, K. Okamoto, H. Hanada, and R. Katoh, *Opt. Lett.*, 2016, **41**, 1498–1501.
6) M. Mitsui, A. Uchida, *Nanoscale* 2024, **16**, 3053−3060.
7) S. Prathapan, S. L. Yang, J. Seth, M. A. Miller, D. F. Bocian, D. Holten, and J. S. Lindsey, *cc*
8) M. R. V. Sahyun, N. Serpone, *J. Phys. Chem. A*, 1997, **101**, 9877–9883.
9) V. Gray, A. Dreos, P. Erhart, B. Albinsson, K. M.-Poulsen, M. Abrahamsson, *Phys. Chem. Chem. Phys*., 2017, **19**, 10931–10939.
10) Rehm, D.; Weller, A. *Ber. Bunsen-Ges. Phys. Chem.* 1969, **73**, 834–839.
11) M. Mitsui, D. Arima, A. Uchida, K. Yoshida, Y. Arai, K. Kawasaki, and Y. Niihori, *J. Phys. Chem. Lett.*, 2022, **13**, 9272–9278.
12) D. Arima and M. Mitsui, *J. Am. Chem. Soc*., 2023, **145**, 6994−7004.